

RESEARCH ARTICLE SUMMARY

PLANT SCIENCE

Brassinosteroid gene regulatory networks at cellular resolution in the *Arabidopsis* root

Trevor M. Nolan[†], Nemanja Vukašinović[†], Che-Wei Hsu[†], Jingyuan Zhang, Isabelle Vanhoutte, Rachel Shahan, Isaiah W. Taylor, Laura Greenstreet, Matthieu Heitz, Anton Afanassiev, Ping Wang, Pablo Szekely, Aiden Brosnan, Yanhai Yin, Geoffrey Schiebinger, Uwe Ohler, Eugenia Russinova*, Philip N. Benfey*

INTRODUCTION: Cells traverse a developmental landscape as they acquire identities and progress toward end-stage differentiation. Gene regulatory networks control this progression and must be tuned according to developmental stage, cell identity, and environmental conditions. Hormones play important roles in remodeling these networks, but it has been challenging to understand how cell identities, developmental states, and hormone responses influence one another. Brassinosteroids are plant steroid hormones that regulate diverse processes, including cell division and cell elongation. Brassinosteroids

signal to activate BRI1-EMS-SUPPRESSOR 1 (BES1) and BRASSINAZOLE-RESISTANT 1 (BZR1) transcription factors, which direct gene regulatory networks to control thousands of genes. Modulating brassinosteroids can lead to different responses depending on the developmental context, but how the underlying gene regulatory networks vary in space and time is unclear.

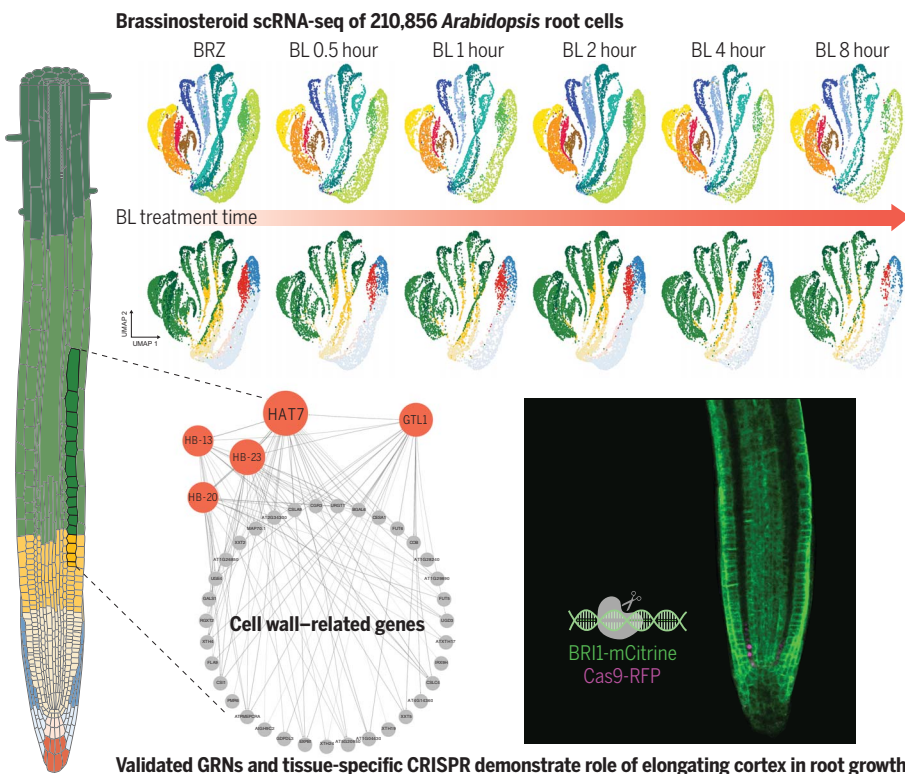
RATIONALE: Single-cell RNA sequencing (scRNA-seq) is a powerful approach to investigate cell- and developmental stage-specific responses to

stimuli, but most previous studies have focused on a single time point. In this work, we used time series scRNA-seq to delineate the gene regulatory networks controlling brassinosteroid response in the *Arabidopsis* root. We then confirmed the spatial and developmental models arising from single-cell analysis using tissue-specific gene manipulations.

RESULTS: We defined brassinosteroid-responsive gene expression using time series scRNA-seq. This identified the elongating root cortex as a site of brassinosteroid-mediated gene expression. Reconstruction of cortex trajectories showed that brassinosteroids promote a shift from proliferation to elongation associated with increased expression of cell wall-related genes. Accordingly, loss of brassinosteroid signaling in the cortex using a tissue-specific CRISPR approach impaired cell expansion in the elongation zone but had little effect on meristem cell length.

To discover regulators of spatiotemporal brassinosteroid responses, we inferred gene regulatory networks across each cell type, developmental stage, and time point of our brassinosteroid time series. Our gene regulatory networks and experimental analysis revealed *HOMEobox FROM ARABIDOPSIS THALIANA 7* (*HAT7*) and *GT-2-LIKE 1* (*GTL1*) as brassinosteroid-responsive transcription factors that regulate cell elongation in the cortex. BES1 and GTL1 interact and control a common set of targets induced by brassinosteroids, as evidenced by misregulation in scRNA-seq of *gtl1 df1* mutants. These datasets represent 210,856 single-cell transcriptomes, providing a high-resolution view of brassinosteroid-mediated gene regulatory networks.

CONCLUSION: We have established the cortex as a site for brassinosteroid-mediated gene expression, where brassinosteroids activate cell wall-related genes and promote elongation. We further showed that *HAT7* and *GTL1* are brassinosteroid-induced regulators along cortex trajectories that control cell elongation. These findings highlight the ability of scRNA-seq to identify context-specific transcription factors, which could be leveraged to precisely engineer plant growth and development. Our results unveil a brassinosteroid signaling network regulating the transition from proliferation to elongation in the cortex, illuminating a spatiotemporal brassinosteroid response. ■



Brassinosteroid networks controlling root cell elongation. scRNA-seq of 210,856 *Arabidopsis* root cells from brassinosteroid treatments and mutants identified the elongating cortex as a site of brassinosteroid response. Gene regulatory networks involving HAT7 and GTL1 family transcription factors induce cell wall-related genes as cells transition to elongation. Tissue-specific CRISPR of *BRASSINOSTEROID INSENSITIVE 1* (*BRI1*) demonstrated the role of the cortex in brassinosteroid-mediated cell elongation. BRZ, Brassinazole; BL, Brassinolide; UMAP, uniform manifold approximation and projection; RFP, red fluorescent protein.

The list of author affiliations is available in the full article online.

*Corresponding author. Email: eugenia.russinova@psb.vib-ugent.be (E.R.); philip.benfey@duke.edu (P.N.B.)

†These authors contributed equally to this work.

Cite this article as T. M. Nolan et al., *Science* **379**, eaf4721 (2023). DOI: 10.1126/science.adf4721

S READ THE FULL ARTICLE AT
<https://doi.org/10.1126/science.adf4721>

RESEARCH ARTICLE

PLANT SCIENCE

Brassinosteroid gene regulatory networks at cellular resolution in the *Arabidopsis* root

Trevor M. Nolan^{1†}, Nemanja Vukašinović^{2,3†}, Che-Wei Hsu^{1,4,5†}, Jingyuan Zhang¹, Isabelle Vanhoutte^{2,3}, Rachel Shahan^{1,6}, Isaiah W. Taylor¹, Laura Greenstreet⁷, Matthieu Heitz⁷, Anton Afanassiev⁷, Ping Wang⁸, Pablo Szekely^{1,6}, Aiden Brosnan¹, Yanhai Yin⁸, Geoffrey Schiebinger⁷, Uwe Ohler^{4,8,9}, Eugenia Russinova^{2,3*}, Philip N. Benfey^{1,6*}

Brassinosteroids are plant steroid hormones that regulate diverse processes, such as cell division and cell elongation, through gene regulatory networks that vary in space and time. By using time series single-cell RNA sequencing to profile brassinosteroid-responsive gene expression specific to different cell types and developmental stages of the *Arabidopsis* root, we identified the elongating cortex as a site where brassinosteroids trigger a shift from proliferation to elongation associated with increased expression of cell wall-related genes. Our analysis revealed *HOMEBOX FROM ARABIDOPSIS THALIANA 7* (*HAT7*) and *GT-2-LIKE 1* (*GTL1*) as brassinosteroid-responsive transcription factors that regulate cortex cell elongation. These results establish the cortex as a site of brassinosteroid-mediated growth and unveil a brassinosteroid signaling network regulating the transition from proliferation to elongation, which illuminates aspects of spatiotemporal hormone responses.

During development, cells pass through different states as they acquire identities and progress toward end-stage differentiation (1). Gene regulatory networks (GRNs) control this progression and must be tuned according to developmental stage, cell identity, and environmental conditions (2–4). Signaling molecules, such as hormones, are central players in coordinating these networks, but it has been challenging to disentangle how cell identities, developmental states, and hormone responses influence one another. Technological advances in single-cell RNA sequencing (scRNA-seq) (2, 5) and tissue-specific gene manipulations (6, 7) make it possible to address this challenge using the *Arabidopsis* root as a model system.

Brassinosteroids are a group of plant steroid hormones that affect cell division and cell elongation during root growth (8–12). Brassinosteroids are sensed at the plasma membrane by BRASSINOSTEROID INSENSITIVE 1 (BRI1) family receptors (13–16), initiating signal transduction events that activate BES1 and BZR1 fam-

ily transcription factors to control thousands of genes (17–20). The brassinosteroid GRN is typically represented singularly without consideration of cell specificity (20–23), even though brassinosteroids lead to different responses depending on the developmental context (24–28).

By profiling brassinosteroid responses across the cell types and developmental stages of the root using scRNA-seq, we discovered that brassinosteroids affect gene expression in the elongating cortex. Reconstruction of cortex trajectories over a scRNA-seq time course showed that brassinosteroids trigger a shift from proliferation to elongation, which is associated with up-regulation of cell wall-related genes. Loss of brassinosteroid signaling in the cortex using tissue-specific CRISPR reduced cell elongation. Our time course data allowed us to propose brassinosteroid-responsive GRNs, which led to the identification of *HAT7* and *GTL1* as validated regulators of brassinosteroid response in the elongating cortex. These datasets represent 210,856 single-cell transcriptomes, providing a high-resolution view of brassinosteroid-mediated GRNs.

scRNA-seq reveals spatiotemporal brassinosteroid responses

To investigate spatiotemporal brassinosteroid responses in the *Arabidopsis* root, we used a sensitized system, which involved inhibiting brassinosteroid biosynthesis using Brassinazole (BRZ) (29) and then reactivating signaling with Brassinolide (BL), the most active brassinosteroid (10, 21, 30) (fig. S1). We treated 7-day-old primary roots for 2 hours with BL or a corresponding mock BRZ control and performed

scRNA-seq on protoplasts isolated from three biological replicates of 0.5-cm root tips (containing meristem, elongation, and early differentiation zones) using the 10X Genomics Chromium system (see materials and methods).

To annotate cell types and developmental stages, we performed label transfer based on our single-cell atlas of the *Arabidopsis* root (31). We distinguished between two domains of the meristem: the proliferation domain, where cells have a high probability of dividing, and the transition domain, where cells divide less frequently but have not yet begun rapid expansion (fig. S2, A to D, and data S2) (32, 33).

After data integration, the 11 major cell types and eight developmental stages identified were logically arranged in two-dimensional (2D) uniform manifold approximation and projection (UMAP) space as previously described for root datasets (fig. S3, A and B) (31, 34). Marker genes characteristic of cell types and developmental stages remained enriched, which suggests that although brassinosteroids alter the expression of thousands of genes, cell identities can be successfully aligned through integration (fig. S3C).

Previous studies have profiled brassinosteroid-responsive gene expression in bulk tissue or in a handful of cell types, conflating cell type and developmental stage (23, 27, 35). To obtain a better spatiotemporal resolution, we performed differential expression analysis for each combination of cell type and developmental stage using pseudobulk expression profiles (materials and methods). We identified 8286 differentially expressed genes (DEGs) (fold-change > 1.5 , false discovery rate < 0.05 ; Fig. 1A and fig. S4, A and B), which were enriched in BES1 and BZR1 targets and had significant overlap with previously identified brassinosteroid-regulated genes (fig. S4C and data S3).

We found that 37% of DEGs were altered in a single cell type or developmental stage and $>82\%$ were differentially expressed in five or fewer cell type–developmental stage combinations (fig. S4B). This indicates that although brassinosteroids broadly influence gene expression, they modulate distinct sets of genes in different spatiotemporal contexts.

Among the tissues with many DEGs was the epidermis, as previously described (9, 12, 24, 27, 35). Atrichoblasts, or nonhair cells in the epidermis, were particularly affected, showing changes across both the meristem and elongation zone. Our data also indicated that brassinosteroids influence gene expression in the cortex, especially in the elongation zone (Fig. 1A and fig. S4A). The cortex has been linked to plant environmental interactions, including response to water limitation (36, 37) and hydrotropism (38, 39). However, it is unknown how brassinosteroids modulate gene expression in this tissue or what processes are affected. To address

*Corresponding author. Email: eugenia.russinova@psb.vib-ugent.be (E.R.); philip.benfey@duke.edu (P.N.B.)

†These authors contributed equally to this work.

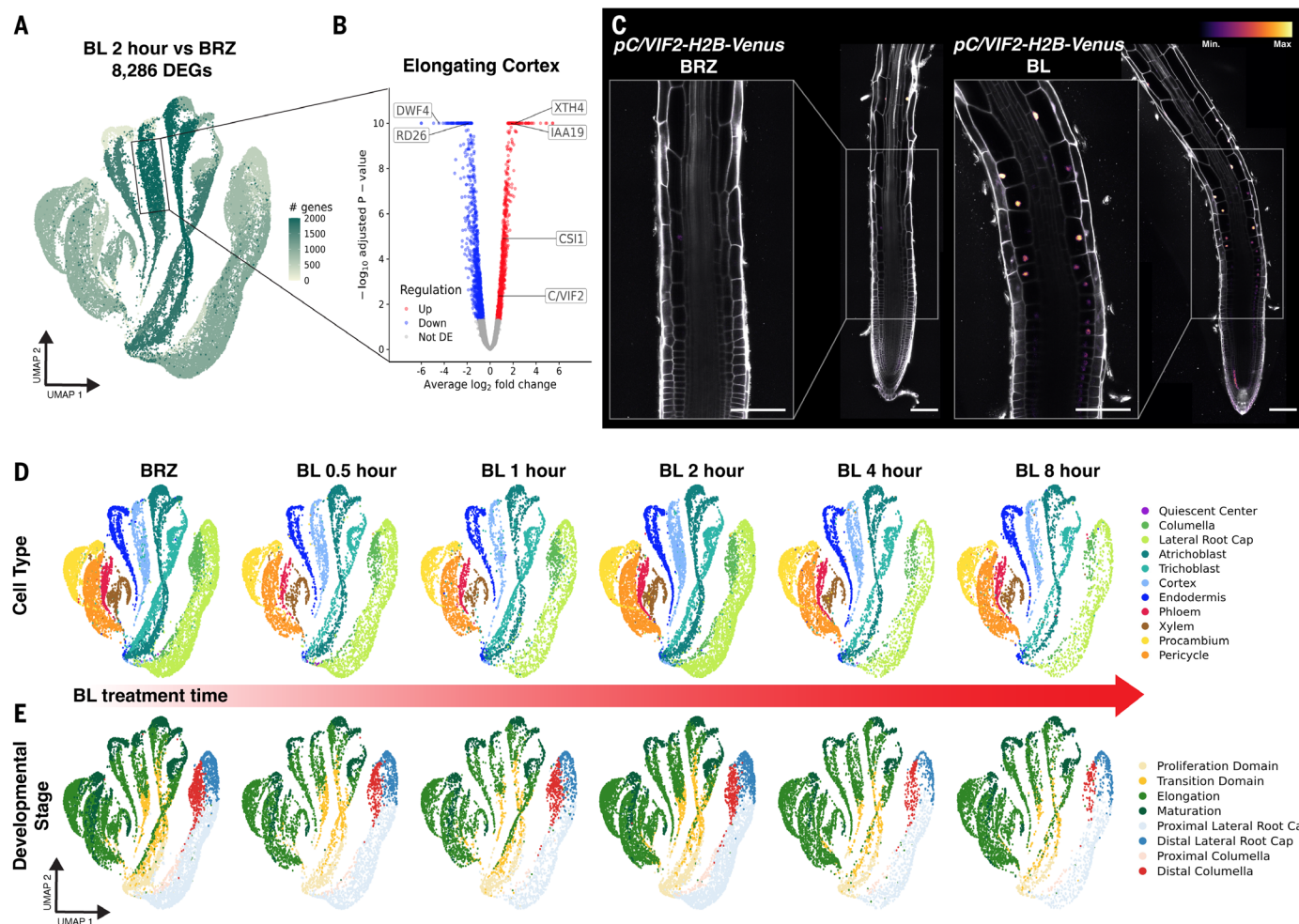


Fig. 1. scRNA-seq identifies brassinosteroid induction of cell wall–related genes in the cortex. **(A)** Spatiotemporal response to 2-hour BL treatment versus BRZ control among each combination of cell type and developmental stage of the *Arabidopsis* root. Color on UMAP projection indicates the number of DEGs. **(B)** Volcano plot of BL DEGs in the elongating cortex. Color indicates the direction of regulation. Known markers of brassinosteroid response, including DWF4, RD26, XTH4, and IAA19, are indicated. C/VIF2 and CSI1 (described in this

study) are also indicated. **(C)** pC/VIF2-H2B-Venus reporter grown on 1 μ M BRZ for 7 days and transferred to 1 μ M BRZ or 100 nM BL for 4 hours. (Inset) C/VIF2 signals in the elongating cortex that increase with BL treatment. Propidium iodide staining is shown in gray, with the color gradient indicating relative C/VIF2-H2B-Venus levels. Scale bars, 100 μ m. **(D)** and **(E)** UMAP of BL treatment scRNA-seq time course. Mock BRZ control represents time 0. Colors indicate cell type (**D**) or developmental stage annotation (**E**).

these questions, we focused on brassinosteroid-mediated gene expression in the elongating cortex.

Brassinosteroids induce cell wall–related genes in the elongating cortex

We found that brassinosteroid treatment led to 967 up-regulated genes and 1156 down-regulated genes in the elongating cortex (Fig. 1B and fig. S4A). Gene ontology (GO) analysis indicated that the up-regulated genes were enriched for genes related to cell wall organization or biogenesis, which is intriguing given the role of brassinosteroids in promoting cell elongation (fig. S4D). The cell wall–related DEGs included *CELLULOSE SYNTHASES* (*CESAs*), *CELLULOSE SYNTHASE INTERACTIVE1* (*CSI1*), and cell wall-loosening enzymes such as *EXPANSINS* and *XYLOGLUCAN ENDOTRANS-*

GLUCOSYLASES. Cell wall–related genes such as *CESAs* have been demonstrated to be direct targets of BES1 and BZR1 (19, 20, 40), but their spatiotemporal regulation, especially in the cortex, has not been reported.

To monitor their responsiveness to brassinosteroids, we generated transcriptional reporters for three of the DEGs with distinct spatiotemporal patterns (Fig. 1C and fig. S5, A to E). For example, *CELL WALL/VACUOLAR INHIBITOR OF FRUCTOSIDASE 2* (*C/VIF2*) was enriched in the transition domain and elongation zone of the cortex and induced by BL (Fig. 1C). These results confirm that our differential expression analysis captures spatiotemporal brassinosteroid responses and raise the possibility that brassinosteroid induction of cell wall–related genes is associated with cortex cell elongation.

Induction of cell wall–related genes is associated with switch to elongation

To better understand how brassinosteroids influence cell wall–related gene expression, we performed scRNA-seq at six time points beginning with BRZ treatment (time 0) and BL treatments for 30 min, 1 hour, 2 hours, 4 hours, and 8 hours (Fig. 1, D and E). These time points capture the rapid root elongation triggered by the readdition of brassinosteroids (35).

Waddington-optimal transport (WOT) is an analytical approach for analyzing expression trends over a scRNA-seq time course. WOT connects snapshots of gene expression to facilitate trajectory reconstruction, identifying putative ancestors for a given set of cells at earlier time points and descendants at later time points (41).

To examine the trajectories leading to the activation of cell wall-related genes in the elongating cortex, we applied WOT (41) and created a cell wall gene signature using 107 cell wall-related genes that were induced by BL in the elongating cortex. We monitored the relative

expression of these genes, resulting in a cell wall score for each cell in the time course (materials and methods). Cortex cells had a higher cell wall score compared with other cell types, which increased with BL treatment (Fig. 2, A and B, and fig. S6, A and B), con-

firms that the cell wall score represents a brassinosteroid-responsive module in the cortex. At the 2-hour BL time point, >20% of cortex cells had a cell wall score greater than 1. By contrast, only 5% or fewer cells in other cell types exhibited scores this high (Fig. 2B). We

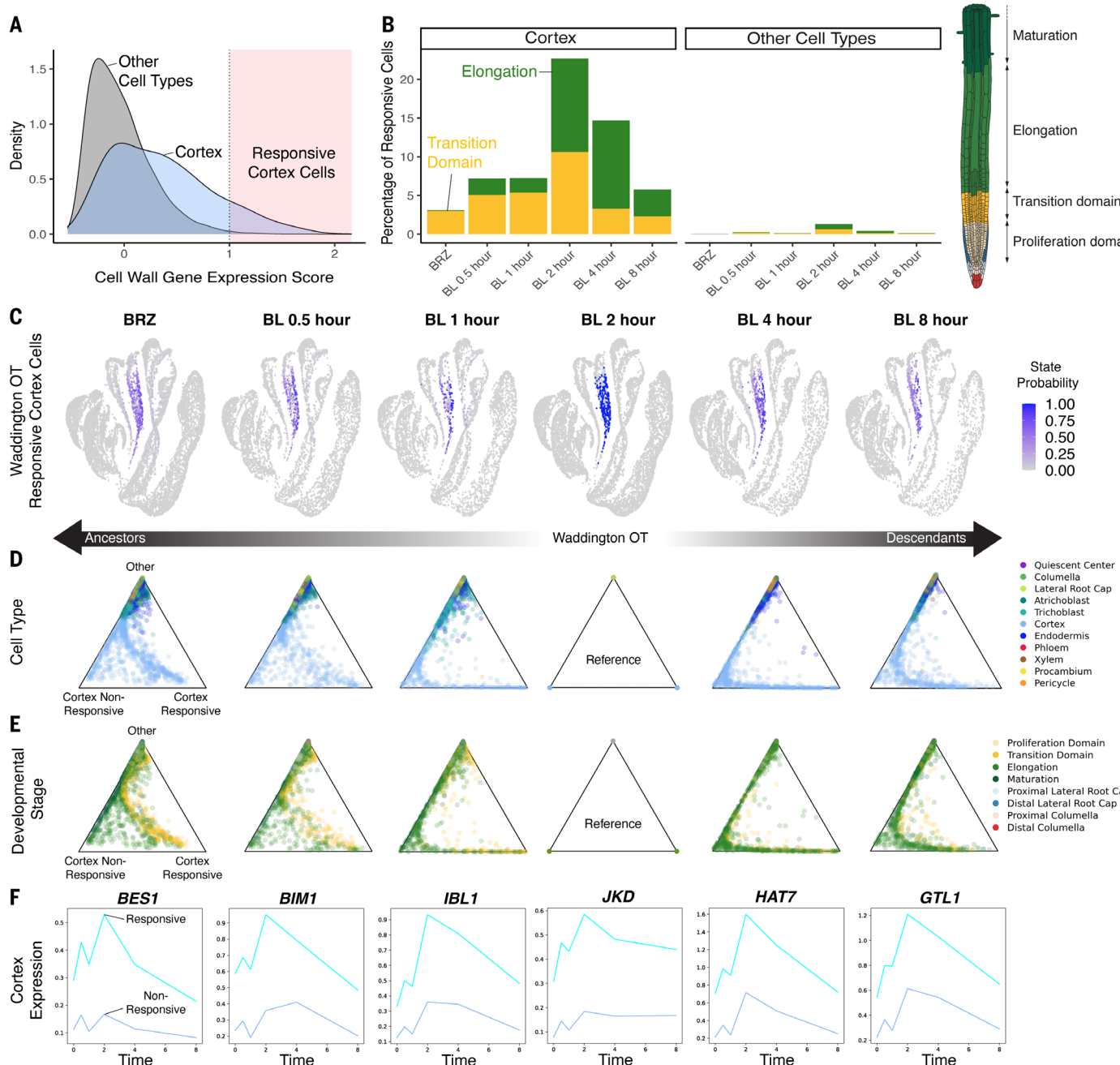


Fig. 2. WOT traces the induction of cell wall–related genes along cortex trajectories associated with the switch to elongation. (A) Density plot showing cell wall gene expression score. The shaded region with cell wall expression scores ≥ 1 indicates responsive cortex cells. (B) Bar plot showing the percentage of responsive cells in the cortex versus other cell types over the time course. Color indicates developmental stage annotation, also depicted in the root schematic. Illustration adapted from the Plant Illustrations repository. Only transition and elongation zones are plotted because other zones represent <2% of responsive

cells. (C) WOT probabilities for cortex responsive state along the BL time course. The BL 2-hour time point was used as a reference; therefore, all cells have a probability of either 1 or 0 at this time point. (D and E) Triangle plots with cells plotted according to WOT cortex responsive, cortex nonresponsive, or other state probabilities for each time point along the BL time course. Color indicates the cell type (D) or developmental stage (E) annotation. (F) Expression trends for select transcription factors differentially expressed along WOT cortex responsive trajectories.

therefore designated cells with a cell wall score of at least 1 as responsive cortex cells to indicate their exceptional brassinosteroid response (Fig. 2A).

An advantage of WOT analysis is that it does not rely on prespecified boundaries between developmental zones. We used this property to examine the relationship between developmental stage annotation and cell wall score. Under BRZ treatment, responsive cortex cells were sparse and predominantly annotated as transition domain. Upon BL treatment, the annotation of responsive cortex cells shifted to the elongation zone (Fig. 2B). Using the cells at the 2-hour time point as a reference, we looked at the probability of cells being ancestors or descendants of responsive cortex cells (Fig. 2C). We also constructed a similar trajectory for the remaining cortex cells, which were designated nonresponsive cortex cells. We visualized these probabilities on barycentric coordinates as triangle plots, where vertices represent a 100% chance of becoming the labeled state and interior positions indicate intermediate probabilities. Cells can be colored according to gene expression, cell types, or other quantities. The cortex nonresponsive state was represented by the lower left vertex, the cortex responsive state was represented by the lower right vertex, and the top vertex represented other states. This illustrated that cortex transition domain cells were predisposed toward the responsive state under BRZ conditions and subsequently shifted from transition domain to elongation zone annotation upon BL treatment (Fig. 2, D and E). These results suggest that brassinosteroids are involved in initiating the elongation of cortex cells through the activation of cell wall-related genes.

WOT trajectories identify brassinosteroid-responsive transcription factors

To reveal potential regulators of cell wall-related genes in the cortex, we performed probabilistic differential expression analysis along WOT trajectories, contrasting cells assigned to cortex responsive versus nonresponsive states at each time point (materials and methods). Among the DEGs identified were known transcription factors in the brassinosteroid pathway, including *BES1* (17), *BES1-INTERACTING MYC-LIKE1* (*BIM1*) (42), and *IBH1-LIKE1* (*IBL1*) (43) (Fig. 2F). We also identified additional transcription factors, including *JACKDAW* (*JKD*), which is involved in ground tissue specification (44); the class I HD-ZIP transcription factor *HAT7* (45, 46); and *GTL1*. Because *JKD* was identified by WOT and a previous BL RNA-seq dataset (21) but not pseudobulk differential expression analysis, we confirmed its brassinosteroid responsiveness (fig. S6, C and D). These results indicate that WOT trajectories can identify brassinosteroid-responsive

transcription factors that may be involved in regulating cell wall-related genes in the cortex.

Analysis of the triple receptor mutant *bri1-T* reveals changes in cortex expression

Because our results indicated that exogenous brassinosteroids lead to the activation of cell wall-related genes in the elongating cortex, we investigated whether this is also the case for endogenous brassinosteroids. A gradient of brassinosteroids is present along the longitudinal axis of the root, with low brassinosteroid levels in the proliferation domain (47). Brassinosteroid biosynthesis increases as cells enter the transition domain and peaks in the elongation zone, shootward of which is a brassinosteroid signaling maximum (35, 47). Interpretation of this endogenous brassinosteroid gradient requires receptor *BRI1* and its homologs *BRL1* and *BRL3* (13, 14, 48–50).

To identify differentially expressed genes, we performed two replicates of scRNA-seq on the brassinosteroid-blind *bri1b1l1b1l3* triple mutant (*bri1-T*) along with paired wild-type (WT) controls (Fig. 3, A to C). A previous study had profiled single cells from *bri1-T*, suggesting potential brassinosteroid responsiveness of the cortex (51). However, these data were from a single replicate, were compared with a WT sample from a different study, and did not resolve developmental stage specificity. By contrast, our analysis across both cell types and developmental stages identified the elongating cortex as exhibiting differential gene expression (Fig. 3, D and E; fig. S7A; and data S3). The genes down-regulated in the elongating cortex of *bri1-T* were enriched for the GO term cell wall organization or biogenesis (fig. S7B). BL treatment increased the proportion of elongating cortex cells (fig. S7C), but fewer elongating cortex cells were observed in *bri1-T* compared with WT (fig. S7D).

To further verify these changes in gene expression, we performed an additional side-by-side scRNA-seq experiment in which we inhibited endogenous brassinosteroids through BRZ treatment. We profiled 16,642 WT control and 14,320 WT BRZ-treated cells and detected 6928 DEGs in BRZ versus control using pseudobulk differential expression analysis of each cell type–developmental stage combination (fig. S8, A to C). Consistent with the idea that brassinosteroids promote cell wall-related gene expression in the elongating cortex, BRZ down-regulated genes in the elongating cortex were enriched for genes associated with cell wall organization or biogenesis (fig. S8D). Together, our analyses of *bri1-T* and BRZ treatment indicate that endogenous brassinosteroid signaling promotes the expression of cell wall-related genes in the cortex associated with the onset of elongation.

The epidermis is widely described as the major site for brassinosteroid-promoted gene

expression in the root (9, 10, 24, 27, 35, 52). Previous studies have shown that epidermal expression of *BRI1* was sufficient to rescue morphological phenotypes, including meristem size of *bri1-T* (9, 24, 53). To determine the extent to which brassinosteroid-regulated gene expression is restored, we performed scRNA-seq on *pGL2-BRI1-GFP/bri1-T* (GFP, green fluorescent protein)—a line in which *BRI1* is expressed in atrichoblast cells of the epidermis of *bri1-T* (9, 27, 53). We identified 8188 DEGs in comparison with WT (Fig. 3F) and 8046 DEGs in comparison with *bri1-T* (Fig. 3G and fig. S9, A to D), which indicates that gene expression remains perturbed (fig. S10, A to D) and that this is far from a complete rescue of the *bri1-T* phenotype.

Tissue-specific CRISPR confirms role of cortex in brassinosteroid-mediated cell expansion

Characterization of cell type–specific brassinosteroid signaling has relied on tissue-specific complementation lines, which has led to conflicting results and has overlooked the role of brassinosteroid signaling in the cortex (9, 24, 27, 35, 51, 53, 54). To selectively block brassinosteroid signaling in cell types of interest, we performed tissue-specific CRISPR (6) of *BRI1*. We used a *bri1* mutant complemented with *pBRI1-BRI1-mCitrine* (Fig. 4A) into which we introduced *Cas9* driven by tissue-specific promoters to knock out *BRI1* either in the epidermis and lateral root cap (*pWER-BRI1-CRISPR*) or in the cortex (*pCO2-BRI1-CRISPR*). mCitrine signals were absent in the expected locations of the tissue-specific CRISPR lines, confirming their efficacy and specificity (Fig. 4, A to C, and fig. S11, A to C).

Because our scRNA-seq data indicated that brassinosteroids promote the expression of cell wall-related genes in the elongating cortex, we hypothesized that loss of brassinosteroid signaling in the cortex would affect final cell size. Indeed, *pCO2-BRI1-CRISPR* lines displayed significantly shorter mature cortex cells, whereas meristematic cortex cell length was relatively unaffected (Fig. 4, D and E).

By contrast, epidermal knockout of *BRI1* in *pWER-BRI1-CRISPR* lines resulted in both reduced meristem cell size and reduced mature cortex cell length (Fig. 4, D and E), which is consistent with the reported role of epidermal brassinosteroid signaling (9, 25, 27, 35, 52) and brassinosteroid responsiveness across developmental zones of the epidermis in our scRNA-seq data.

We measured the cell width of the tissue-specific CRISPR lines and found that *pWER-BRI1-CRISPR* lines have significantly wider cortex cells. However, despite their reduced cortex cell length, *pCO2-BRI1-CRISPR* lines did not have increased cell width (fig. S11D). This prompted us to perform 3D cell segmentations using MorphoGraphX (55, 56). We found that

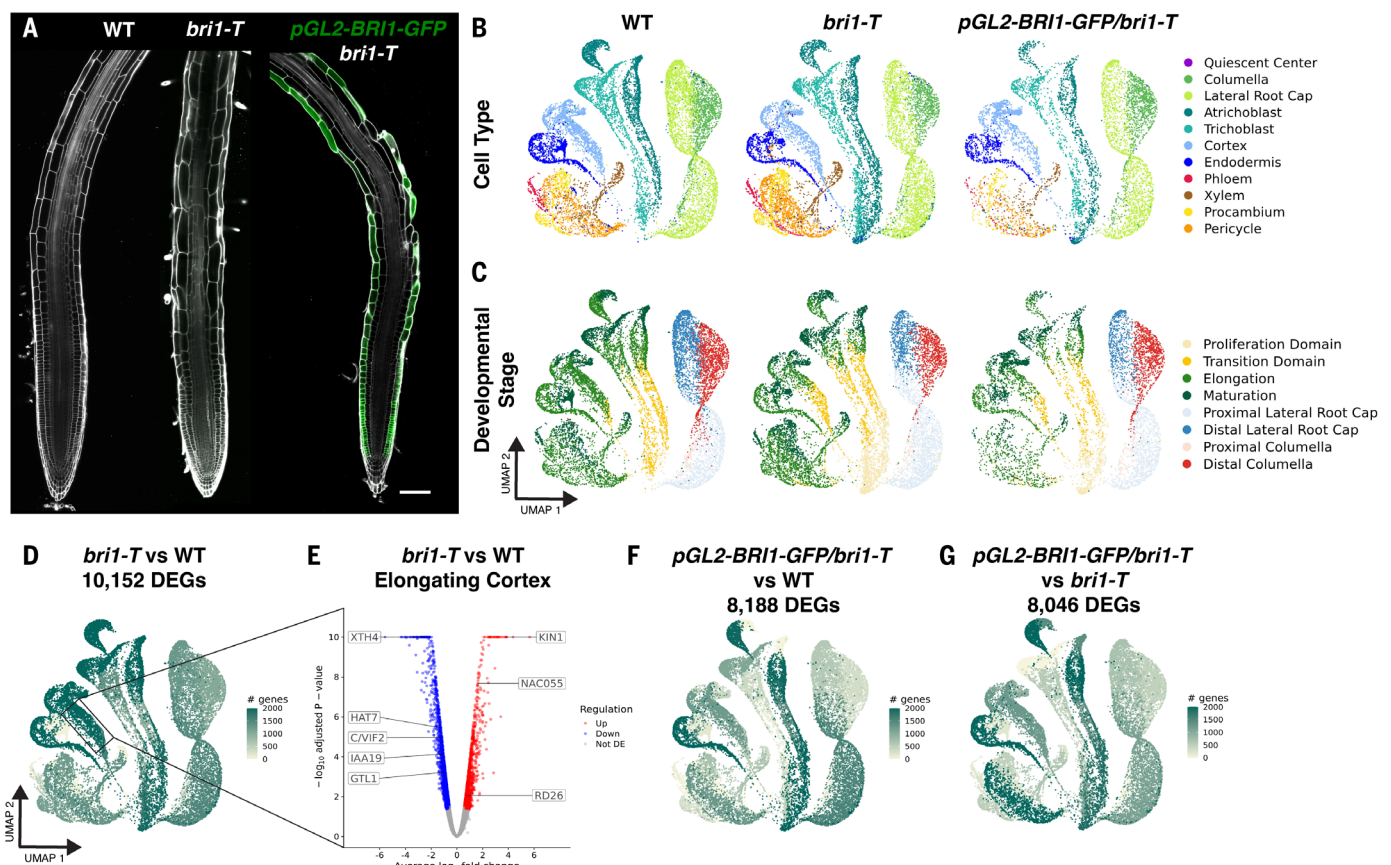


Fig. 3. Triple receptor mutant *bri1-T* gene expression changes in cortex and distinct patterns in *pGL2-BRI1-GFP/bri1-T*. **(A)** Seven-day-old WT, *bri1-T*, and *pGL2-BRI1-GFP/bri1-T* roots grown under control conditions. Propidium iodide staining is shown in gray, and GFP is shown in green. Scale bar, 100 μ m. **(B)** UMAP projection of scRNA-seq from 14,334 WT cells, 12,649 *bri1-T* cells, and 7878 *pGL2-BRI1-GFP/bri1-T* cells. Two biological replicates of scRNA-seq were performed for each genotype. Colors indicate cell type annotation. **(C)** UMAP

projection colored by developmental stage annotation. **(D)** UMAP colored by DEGs for each cell type–developmental stage combination of *bri1-T* compared with WT. **(E)** Volcano plot of DEGs in the elongating cortex from *bri1-T* compared with WT showing down-regulation of cell wall-related genes in *bri1-T*. Color indicates the direction of regulation. **(F and G)** UMAPs colored by DEGs for each cell type–developmental stage combination of *pGL2-BRI1-GFP/bri1-T* compared with WT (F) or *pGL2-BRI1-GFP/bri1-T* compared with *bri1-T* (G).

the cortex cell volume was reduced in *pCO2-BRI1-CRISPR* roots but increased in *pWER-BRI1-CRISPR* roots (fig. S12, A and B). Brassinosteroids primarily control cell elongation rather than cell volume when signaling is affected across the entire root (51, 52). Alternatively, the changes in volume observed in the tissue-specific CRISPR lines could be the result of constraints between tissues or tissue-specific functions of brassinosteroids in influencing cell volume. These results indicate that in addition to the epidermis, brassinosteroid signaling in the cortex is required to promote cell expansion in the elongation zone. The cortex could instruct anisotropic growth through its physical connection with the epidermis, but as the outermost tissue, relaxation of the epidermis appears to be required to allow for cell elongation (57, 58). This may explain the widening of cortex cells in *pWER-BRI1-CRISPR* lines.

BRI1 was also reported to rescue *bri1-T* morphology when expressed in the developing phloem using the *CVP2* promoter (51, 53, 54). However, gene expression was not fully restored to WT

levels in either epidermal or phloem rescue lines. Our scRNA-seq of epidermal *pGL2-BRI1-GFP/bri1-T* lines showed gene expression patterns distinct from either WT or *bri1-T*. Similarly, scRNA-seq of *pCVP2-BRI1-CITRINE/bri1-T* indicated an intermediate state between WT and *bri1-T* (51). *BRI1* driven by its native promoter was still present in the stele of our tissue-specific CRISPR lines when we observed phenotypic defects, suggesting that, unlike *pCVP2-BRI1*, native expression of *BRI1* in the stele is not sufficient for brassinosteroid-induced cell elongation and root growth. These results confirm the role of the epidermis in brassinosteroid-regulated root growth and reveal the function of the cortex in brassinosteroid-mediated cell elongation, demonstrating how scRNA-seq can identify a spatiotemporal context for hormone signaling.

***HAT7* and *GTL1* are brassinosteroid-responsive regulators along cortex trajectories**

To define a core set of genes associated with brassinosteroid response along cortex trajec-

tories, we first compared genes induced in the cortex by BL treatment with those down-regulated in the cortex of *bri1-T*. Of the 768 genes in common, we then examined which vary with development in WT cortex trajectories (31). The intersection of these three lists identified a core set of 163 brassinosteroid-responsive DEGs (Fig. 5A and data S3). Consistent with regulation by brassinosteroids, 69% of the core DEGs are BES1 and BZR1 direct targets from chromatin immunoprecipitation (ChIP) experiments (19, 20, 59). Expression along cortex pseudotime illustrates induction by BL treatment and down-regulation in *bri1-T* (Fig. 5B). *HAT7* and *GTL1* were induced along these trajectories, suggesting a potential role for these transcription factors in controlling brassinosteroid-regulated gene expression in the cortex (Fig. 5, C to E).

To gain insight into their roles, we generated translational reporter lines for *HAT7* and *GTL1*. Under control conditions, *pHAT7-HAT7-mCitrine* lines showed expression in the transition domain and elongation zone of the cortex

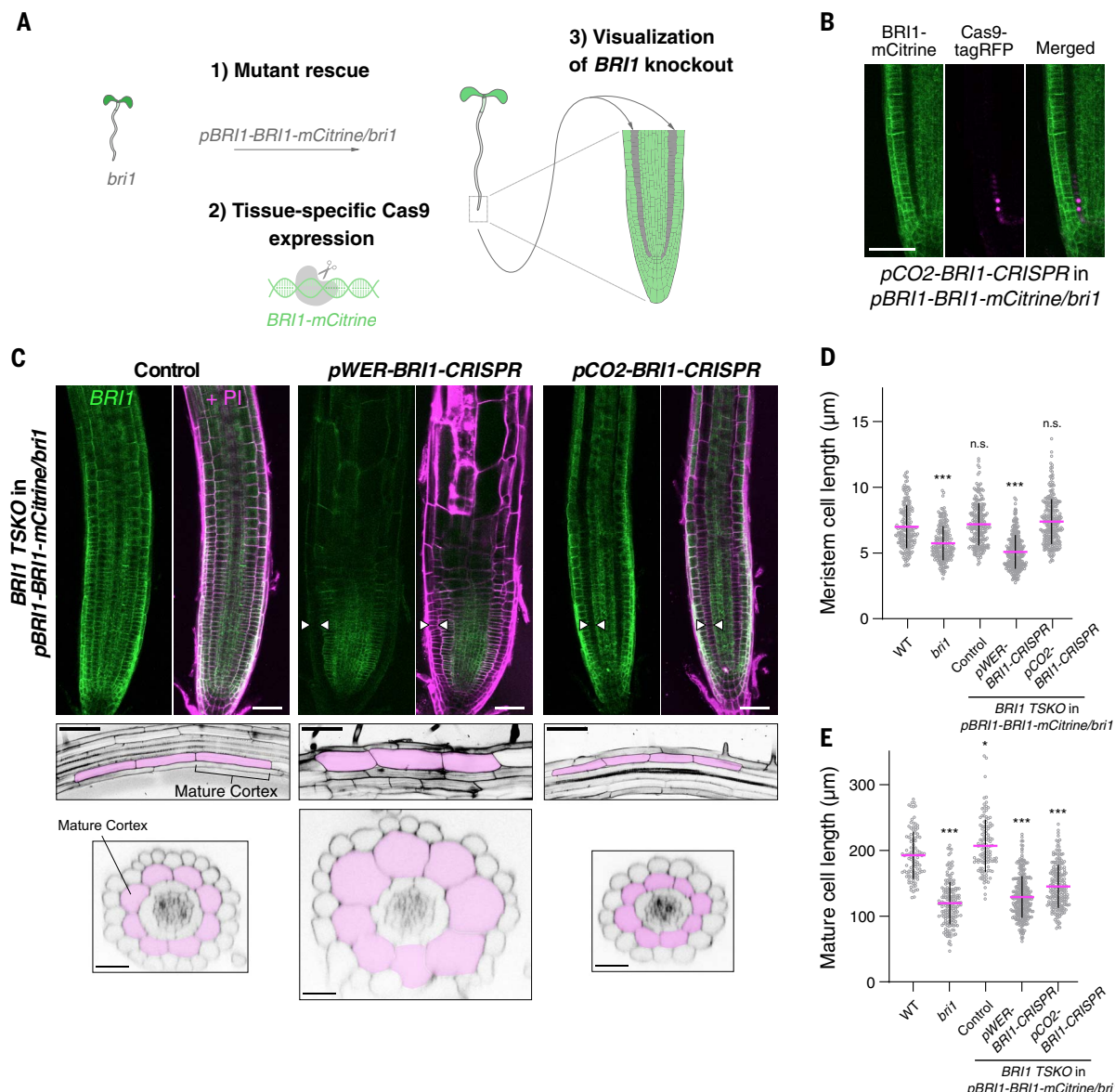


Fig. 4. Tissue-specific CRISPR of *BRI1* confirms role for cortex in brassinosteroid-mediated cell expansion. (A) Overview of *BRI1* tissue-specific CRISPR approach. A *bri1* mutant complemented with *pBRI1-BRI1-mCitrine* (1) was used as background to introduce tissue-specific Cas9 along with gRNAs targeting *BRI1* (2). This allows for visualization of *BRI1* knockout in specific cell layers, such as the cortex, when *pCO2-BRI1-CRISPR* is used (3). (B) Appearance of Cas9-tagRFP in the cortex is associated with loss of *BRI1-mCitrine* signal, confirming tissue-specific knockout. RFP, red fluorescent protein. Scale bar, 50 μm. (C) Confocal images of *BRI1* tissue-specific CRISPR lines. Control indicates a broad expression pattern of *BRI1-mCitrine* in *pBRI1-BRI1-mCitrine/bri1*. *BRI1-mCitrine* signals are shown in green and propidium iodide staining (PI) in magenta (top). White arrows specify tissues with absence of *BRI1-mCitrine* signal; epidermis for *pWER-BRI1-CRISPR* and cortex for

pCO2-BRI1-CRISPR. Mature root longitudinal and cross sections illustrate changes in cell length (middle) and width (bottom), respectively. Cortex cells are pseudocolored to indicate their position. Scale bars, 50 μm (top), 100 μm (middle), and 25 μm (bottom). (D) Quantification of meristematic cortex cell length, defined as the first 20 cells of individual roots starting from the quiescent center. Control indicates *pBRI1-BRI1-mCitrine/bri1* complemented line. (E) Quantification of mature cortex cell length. For (D) and (E), all individual data points are plotted. Magenta horizontal bars represent the means, and error bars represent SDs. Significant differences between each line and WT were determined by one-way analysis of variance (ANOVA) and Dunnett's multiple comparison tests. ***P < 0.001; **P < 0.01; *P < 0.05; n.s., not significant. TSKO, tissue-specific knockout.

(Fig. 5F). We also observed HAT7 signals in the epidermis and endodermis, in line with expression patterns in our WT scRNA-seq atlas (31). *HAT7* expression was decreased when brassinosteroid biosynthesis was inhibited with BRZ and restored upon BL treatment (fig. S13A).

pGTL1-GTL1-mCitrine was more broadly expressed, with increasing levels in the cortex as

cells progress from the transition domain to the elongation zone (Fig. 5G). *GTL1-mCitrine* expression was reduced by BRZ and increased by BL treatment (fig. S13B). These results confirm that brassinosteroids promote the expression of *HAT7* and *GTL1*, coinciding with the onset of cell elongation. Furthermore, *HAT7* and *GTL1* are direct targets of BES1 and BZR1

(19, 20, 59), which suggests that they may be part of the brassinosteroid-directed GRN activated as cells progress from proliferation to elongation.

Previous studies have inferred global (19, 20, 22, 23) or temporally resolved GRNs (21) for brassinosteroid response, but they have lacked cell type and developmental stage

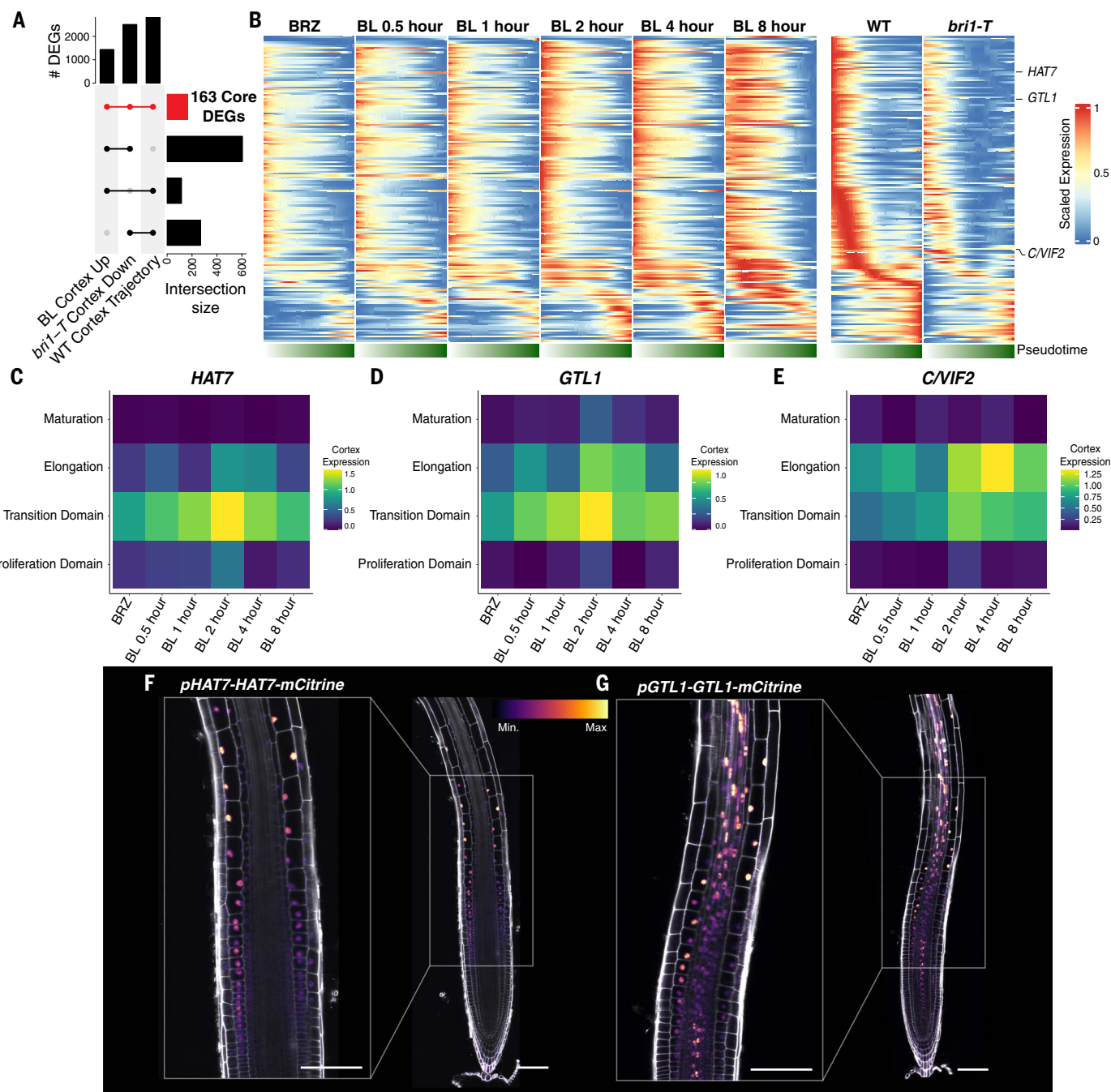


Fig. 5. *HAT7* and *GTL1* are brassinosteroid-responsive regulators along cortex trajectories. (A) Upset plot showing a comparison of genes up-regulated by BL in the cortex, down-regulated in the cortex of *bri1-T*, and differentially expressed along WT cortex trajectories. The red color indicates 163 genes common to all three sets. (B) Gene expression trends for 163 core brassinosteroid DEGs along cortex trajectories. Scaled expression along cortex pseudotime is plotted for each time point of the brassinosteroid time series and for WT versus *bri1-T*. Lower bar indicates pseudotime progression

calculated by CytoTRACE. (C to E) Gene expression trends for *HAT7* (C), *GTL1* (D), and *C/VIF2* (E) along the developmental zones of the cortex for each time point of the brassinosteroid time course. Color bars indicate the scaled expression level in the cortex. (F and G) Seven-day-old roots expressing *pHAT7-HAT7-mCitrine* (F) or *pGTL1-GTL1-mCitrine* (G) reporters under control conditions show an increased expression as cortex cells elongate. Propidium iodide staining is shown in gray, with the color gradient indicating relative mCitrine levels. Scale bars, 100 μm.

specificity. To infer GRN configurations across our brassinosteroid time series, we used CellOracle (materials and methods), focusing on BL DEGs and associated transcription factors.

Analysis of network importance scores, such as centrality measures, is a powerful approach to prioritize candidate regulators among DEGs (60). Because the cell wall signature peaked at 2 hours after BL treatment, we prioritized

transcription factors with high network centrality scores in the elongating cortex at this time point. *HAT7* was the top-ranked transcription factor in terms of degree centrality. *HB13*, *HB20*, and *HB23* were also among the top 10

transcription factors (Fig. 6, A and B, and data S4).

We used CRISPR to generate *hat7* loss-of-function mutants but did not observe phenotypes concerning cortex cell elongation (fig. S14, A to C). Together HAT7, HB13, HB20, and HB23 make up the alpha clade HD-ZIP I transcription factors (45, 46, 61–65). Because *HB13*, *HB20*, and *HB23* are induced by brassinosteroids and are predicted to regulate cell wall-related genes in our GRNs (Fig. 6B; fig. S15, A and B; and data S5), we next generated *hat7 hb13 hb20 hb23* quadruple mutants through

multiplex CRISPR. Mature cortex cell length was reduced by ~25% in two independent quadruple mutants (Fig. 6, C and D, and fig. S16, A to C), providing evidence that HAT7 and its homologs are required for cell elongation. *hat7 hb13 hb20 hb23* quadruple mutants also had wider mature cortex cells (fig. S16C) with increased volume compared with WT (fig. S17, A and B). Despite the decrease in final cell length, the root length of the quadruple mutant was not reduced (fig. S14A), which suggests that the decrease in cell length is at least partially compensated for by increased cell pro-

duction. We found that *hat7 hb13 hb20 hb23* quadruple mutants have an average of 15 more meristematic cortex cells compared with WT (fig. S16B), which is consistent with a compensatory increase in proliferation.

We next investigated GTL1, the fifth-highest-ranked transcription factor in the BL 2-hour elongating cortex GRN (Fig. 6, A and B). Given that GTL1 was shown to function redundantly with DF1 in terminating root hair growth (66, 67), we examined *gtl1 df1* double mutants and found shorter mature cortex cell lengths and shorter roots compared with WT (Fig. 6,

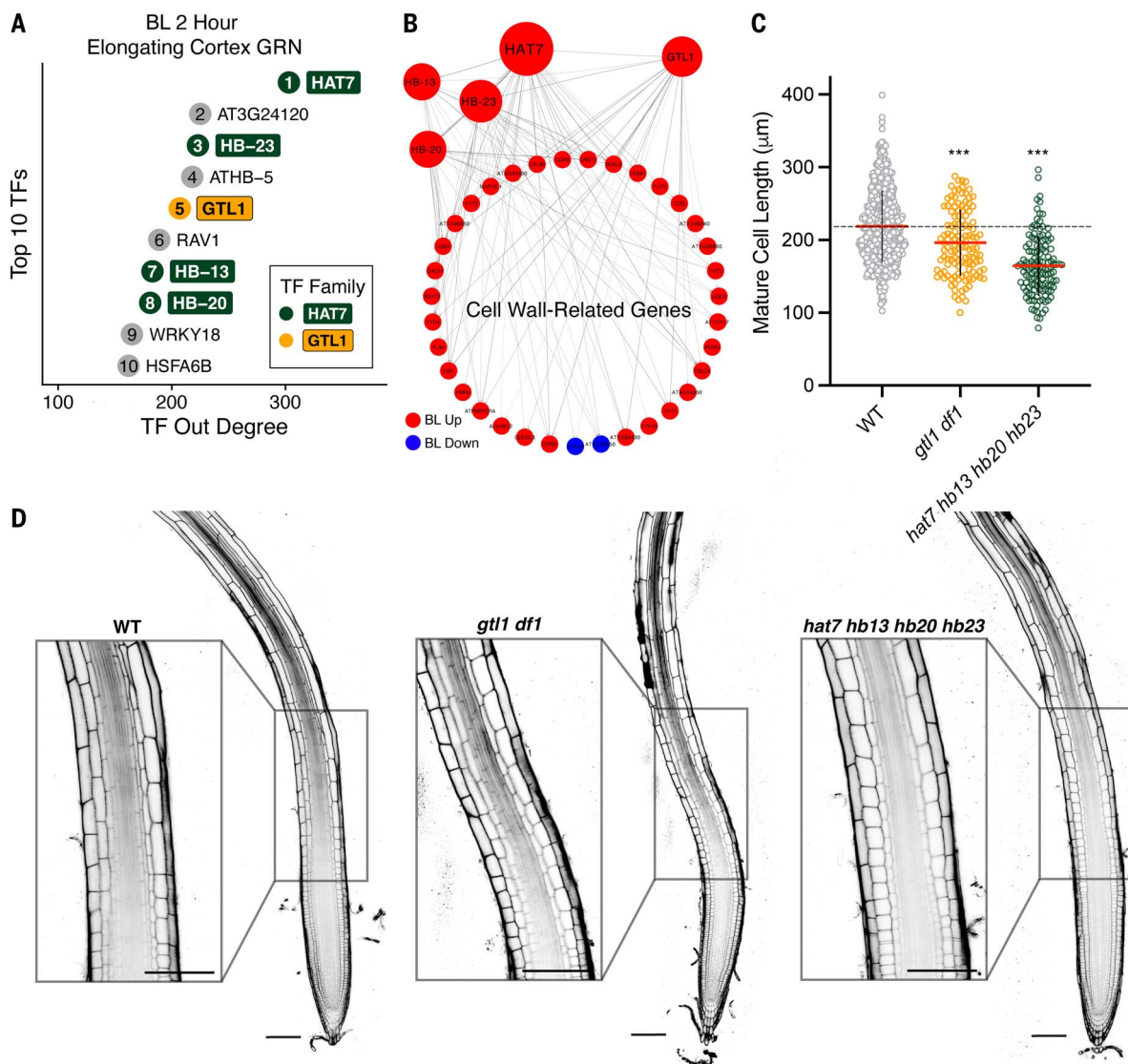


Fig. 6. HAT7 and GTL1 are top-ranked regulators in cortex GRNs and affect brassinosteroid-related phenotypes. (A) Top 10 transcription factors (TFs) in the CellOracle BL 2-hour elongating cortex GRN ranked by out-degree. Ranking is indicated by the number inside the circle. Color indicates transcription factor family, with light gray corresponding to any family other than HAT7 or GTL1. (B) Subnetwork showing cell wall-related genes that are predicted targets of HAT7 and GTL1 in the CellOracle elongating cortex GRN. HB13, HB20, and HB23 are included in the subnetwork

because they are connected to HAT7 and cell wall-related genes. Node size is proportional to degree. (C) Quantification of mature cortex cell length. Red horizontal bars represent the means, and error bars represent SDs. Significant differences between each line and WT were determined by one-way ANOVA and Dunnett's multiple comparison tests. *** $P < 0.001$. (D) Propidium iodide staining of 7-day-old WT, *hat7 hb13 hb20 hb23*, and *gtl1 df1* roots. Insets show cortex cells entering the elongation zone. Scale bars, 100 μm.

C and D, and fig. S14, A to C). *DF1* was challenging to detect in scRNA-seq (fig. S15A) because of its low expression level (66). However, we observed increasing trends of *DF1* expression along WOT trajectories in the BL time course, especially in cell wall-responsive cortex cells (fig. S15B), which was verified using a *pDF1-DF1-GFP* reporter (fig. S15C).

We examined the overlap between our CellOracle BL 2-hour elongating cortex GRN and a GRN reported by Clark *et al.* from bulk RNA-seq data in response to brassinosteroids (21). Only 43/31,330 edges are shared between the two networks. Moreover, HAT7, HB13, HB20, HB23, and GTL1 were among the top 10 transcription factors in terms of out-degree in the CellOracle elongating cortex GRN, which we validated through mutant analysis. However, none of these were among the top 100 transcription factors in the Clark *et al.* GRN (fig. S18, A and B), which suggests that they would have been difficult to prioritize from the bulk data alone. Together, our genetic analysis of HAT7 and GTL1 family transcription factors illustrates the power of GRN-mediated discovery of regulatory factors in spatiotemporal brassinosteroid response.

BES1 and GTL1 physically interact and regulate shared target genes

Because BES1 is known to interface with other transcription factors in controlling brassinosteroid-regulated gene expression, we compared target genes for BES1 and BZR1 (19, 20, 59) with ChIP targets of GTL1 and DF1 (66). BES1 and BZR1 share 3020 common targets with GTL1 and 2490 common targets with DF1 (fig. S19A). When compared with brassinosteroid-regulated genes from scRNA-seq, BES1 and GTL1 targets showed the strongest enrichment in genes up-regulated by brassinosteroids in the transition domain and elongation zone of the cortex (fig. S19B), with 297 common targets of both BES1 or BZR1 and GTL1 being induced in the elongating cortex by BL treatment.

Given the overlap between BES1 and GTL1 targets, we hypothesized that these transcription factors physically interact to regulate a common set of genes. Coimmunoprecipitation showed that GTL1-FLAG pulled down BES1-GFP (fig. S19C). These results suggest that brassinosteroids induce GTL1 and subsequently BES1 and GTL1 interact to control a common set of target genes. This type of feed-forward loop could provide a mechanism to amplify the brassinosteroid signal and/or to direct BES1 to drive tissue-specific gene expression by interacting with other more specifically expressed transcription factors.

In addition to *GTL1*, we found that previously described BES1 interacting transcription factors, including *BRASSINOSTEROIDS AT VASCULAR AND ORGANIZING CENTER*

(*BRAVO*) (26), *BIM1* (42), and *MYB30* (68), were differentially expressed in our scRNA-seq datasets in response to BL (data S3). Among these, *MYB30* was enriched in atrichoblasts of the epidermis and induced by BL treatment (fig. S20, A and B). CellOracle correctly predicted that *MYB30* regulates *LTPG2*, a known target of *MYB30* (69), which also showed enrichment in atrichoblasts and temporal induction in response to brassinosteroids after *MYB30* activation (fig. S20B). This supports the idea that cell type-specific patterns of brassinosteroid response may be at least partially explained by interactions between BES1 or BZR1 and other transcription factors.

scRNA-seq reveals cell type-specific expression underlying *gtl1 df1* phenotypes

Our results indicate that *gtl1 df1* mutants have reduced cortex cell elongation. However, *gtl1 df1* mutants have longer trichoblasts (66). A downstream regulatory network that enables GTL1-mediated growth inhibition has been dissected in trichoblasts (66, 67). To identify the cell type-specific changes in gene expression underlying *gtl1 df1* cortex phenotypes, we performed scRNA-seq on *gtl1* and *df1* single mutants and the *gtl1 df1* double mutant. Using pseudobulk differential expression analysis, we detected relatively subtle changes in *gtl1* or *df1* single mutants compared with the WT (fig. S21, A to C). By contrast, 8391 genes were differentially expressed in *gtl1 df1* double mutants versus WT (Fig. 7A).

In total, 1077 genes were up-regulated across all developmental stages of the cortex of *gtl1 df1*, and 947 genes were down-regulated. Most cortex DEGs were affected in the elongation zone (Fig. 7, A and B; fig. S21C; and data S3). Of the down-regulated genes in the cortex of the double mutant, 226 genes were also up-regulated by BL treatment. Furthermore, 31.3% of the core brassinosteroid DEGs were down-regulated in the cortex of *gtl1 df1*, whereas only 6.8% were up-regulated (data S3). These results suggest that GTL1 and DF1 promote the expression of a subset of brassinosteroid-induced genes in the cortex.

Plotting *gtl1 df1* DEGs along cortex pseudotime illustrated the down-regulation of several genes involved in cell elongation, including *CESA5* and *AHA2* (Fig. 7C). These genes were enriched for the GO term cell wall organization or biogenesis (fig. S21D). We next examined *C/VIF2* because it is induced by BL in the cortex, but its expression decreased in cortex cells of *gtl1 df1* (Fig. 7, D and E). A *pC/VIF2-H2B-Venus* reporter showed expression of *C/VIF2* in the transition and elongation zone of the WT cortex, whereas its expression was reduced in the cortex of *gtl1 df1* mutants (Fig. 7F and movie S1). The reduced expression of cell wall-related genes in *gtl1 df1* mutants validates our cell type-specific brassinoste-

roid GRNs and identifies a function of GTL1 in promoting cortex cell elongation in response to brassinosteroids.

Discussion

Understanding how hormone-mediated GRNs are controlled in space and time has the potential to enable the engineering of specific downstream responses to optimize plant growth under a changing environment (10, 70). Plant hormones, including brassinosteroids, auxin, gibberellins, and abscisic acid, have been shown to exhibit tissue-specific responses (71–76), but how the associated GRNs are modulated in different cell types at particular developmental stages is enigmatic. In this study, we profiled brassinosteroid responses across cell types, developmental stages, and time points of treatment using scRNA-seq, providing a high-resolution map of signaling outputs. These data are publicly available as an interactive browser (<https://shiny.mdc-berlin.de/ARVEX/>). We identified the elongating cortex as a spatiotemporal context for brassinosteroid signaling, where brassinosteroids activate cell wall-related genes and promote elongation. We further showed that HAT7 and GTL1 are brassinosteroid-induced regulators along cortex trajectories that control cell elongation. These findings highlight the ability of single-cell genomics to identify context-specific transcription factors, a capability that could be leveraged to precisely engineer plant growth, development, and responses to stress. Our results reveal spatiotemporal brassinosteroid responses and the underlying GRNs.

Materials and methods summary

Arabidopsis accession Columbia-0 (Col-0) was used as a WT. The following lines have been previously described: *bri1 GABI_134E10* (77); *bri1-116bri1bri1* triple mutant (*bri1-T*) (50); *pGL2-BRI1-GFP/bri1-T* (27); *gtl1-1* (WiscDsLox413-416C9), *df1-1* (SALK_106258), and *gtl1-1 df1-1* (66); and JKD-Ypet recombineering line (44). We produced *hat7* single mutants and *hat7 hb13 hb20 hb23* quadruple mutants using FASTRED multiplex CRISPR constructs containing an intronized version of Cas9 (78, 79).

scRNA-seq experiments were performed as previously described (31). For each sample, ~0.5-cm root tips from 7-day-old plants were harvested and digested with protoplasting solution, and 16,000 cells were loaded on a 10X Genomics Chromium instrument, with the aim to capture 10,000 cells per sample with the 10X Genomics Chromium 3' Gene expression v3 or v3.1 kits.

For BL scRNA-seq, we first grew plants on 1 μ M BRZ to deplete endogenous brassinosteroids, then transferred plants to either a fresh BRZ plate or 100 nM BL. We performed two separate BL scRNA-seq treatment experiments. The first pilot experiment consisted of a BRZ

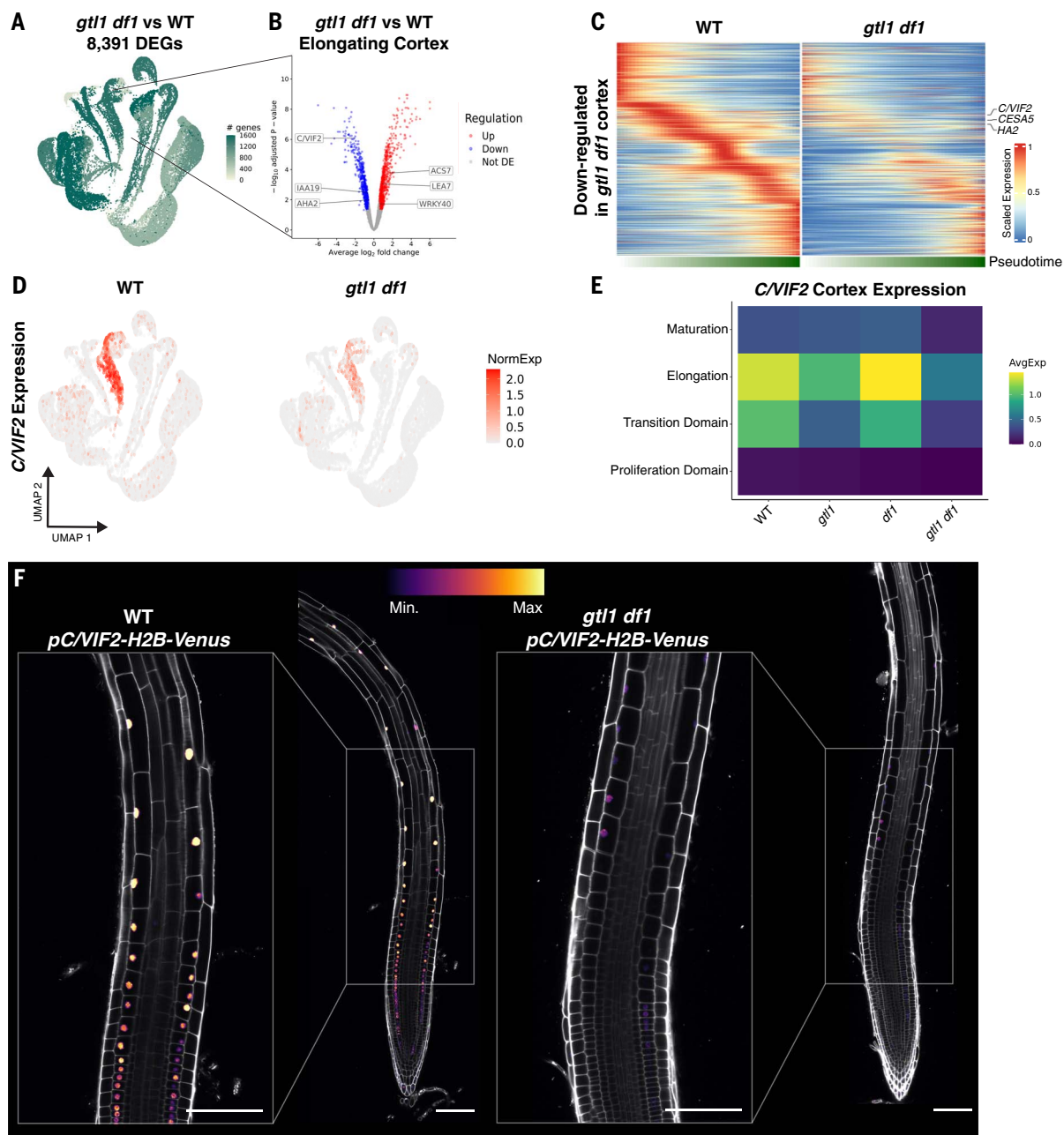


Fig. 7. scRNA-seq reveals cell type–specific expression underlying *gtl1 df1* phenotypes. (A) UMAP projection of scRNA-seq from 74,810 WT, *gtl1*, *df1*, and *gtl1 df1* cells. Two biological replicates were profiled for each genotype. Color indicates DEGs for each cell type–developmental stage combination of *gtl1 df1* compared with WT. (B) Volcano plot of DEGs in the elongating cortex from *gtl1 df1* compared with WT. Color indicates the direction of regulation. (C) Gene expression trends along cortex trajectories for down-regulated DEGs in *gtl1 df1* compared with WT. Each row represents the scaled expression of a gene along

cortex pseudotime. The lower bar indicates pseudotime progression calculated by CytoTRACE. (D) Expression of *C/VIF2* in WT and *gtl1 df1* scRNA-seq. The color scale represents log normalized, corrected UMI counts. (E) *C/VIF2* expression levels plotted along the developmental zones of the cortex for WT, *gtl1*, *df1*, and *gtl1 df1*. The color bar indicates the scaled expression level. (F) Seven-day-old root images of a *pC/VIF2-H2B-Venus* reporter in WT or *gtl1 df1* under control conditions. Propidium iodide staining is shown in gray, with the color gradient indicating relative mCitrine levels. Scale bars, 100 μ m.

and 2-hour BL treatment. The second experiment included two additional BRZ and BL 2-hour replicates and a single replicate of the other time points in our time course (BL 0.5-, 1-, 4-, and 8-hour treatments). Each of the BL treatments was staggered so that all samples

were collected simultaneously. A total of 70,223 cells were recovered from the BL treatment scRNA-seq experiments. WT, *bri1-T*, and *pGL2-BR1-GFP/bri1-T* were similarly profiled in a side-by-side scRNA-seq experiment under control conditions with two replicates per geno-

type, resulting in 34,861 cells. To test the effect of inhibiting endogenous brassinosteroid biosynthesis, we grew WT on 1 μ M BRZ or a mock dimethyl sulfoxide (DMSO) control and performed two replicates of scRNA-seq spanning 30,962 cells for BRZ versus control analysis.

Finally, scRNA-seq was performed on WT, *gtl1*, *df1*, and *gtl1 df1* in duplicate under control conditions, resulting in 74,810 scRNA-seq expression profiles.

scRNA-seq data were aligned against the *Arabidopsis* TAIR10 reference genome. Quality filtering of cells was performed using the R package COPilot (Cell preProOcessing Pipeline kaListO busTools) (31, 80). Downstream analyses were carried out using Seurat version 3.1.5 (81), WOT (41), muscat (82), tradeSeq (83), and GRNs inferred using CellOracle (60).

To selectively block brassinosteroid signaling in cell types of interest, we performed tissue-specific CRISPR (6) of *BRI1* in a *brl1* mutant complemented with *pBRII-BRI1-mCitrine*. Two guide RNAs (gRNAs) targeting *BRI1* were simultaneously expressed along with tissue-specific Cas9 to knock out *BRI1* either in the epidermis and lateral root cap (*pWER-BRI1-CRISPR*) or in the cortex (*pCO2-BRI1-CRISPR*). For each root used for quantitative analysis, *BRI1-mCitrine* signal was acquired to confirm the efficiency of the tissue-specific knockout system. The supplementary materials provide complete details of the materials and methods, including those summarized above.

REFERENCES AND NOTES

- E. Pierre-Jerome, C. Drapek, P. N. Benfey, Regulation of Division and Differentiation of Plant Stem Cells. *Annu. Rev. Cell Dev. Biol.* **34**, 289–310 (2018). doi: 10.1146/annurev-cellbio-100617-062459; pmid: 30134119
- R. Shahani, T. M. Nolan, P. N. Benfey, Single-cell analysis of cell identity in the *Arabidopsis* root apical meristem: Insights and opportunities. *J. Exp. Bot.* **72**, 6679–6686 (2021). doi: 10.1093/jxb/erab228; pmid: 34018001
- M. Levine, E. H. Davidson, Gene regulatory networks for development. *Proc. Natl. Acad. Sci. U.S.A.* **102**, 4936–4942 (2005). doi: 10.1073/pnas.0408031102; pmid: 15788537
- M. A. Moreno-Risueno, W. Busch, P. N. Benfey, Omics meet networks – using systems approaches to infer regulatory networks in plants. *Curr. Opin. Plant Biol.* **13**, 126–131 (2010). doi: 10.1016/j.pbi.2009.11.005; pmid: 20036612
- C. Seyffert et al., Advances and Opportunities in Single-Cell Transcriptomics for Plant Research. *Annu. Rev. Plant Biol.* **72**, 847–866 (2021). doi: 10.1146/annurev-arpplant-081720-010120; pmid: 33730513
- W. Decaeester et al., CRISPR-TSKO: A Technique for Efficient Mutagenesis in Specific Cell Types, Tissues, or Organs in *Arabidopsis*. *Plant Cell* **31**, 2868–2887 (2019). doi: 10.1105/tpc.19.00454; pmid: 31562216
- X. Wang et al., An inducible genome editing system for plants. *Nat. Plants* **6**, 766–772 (2020). doi: 10.1038/s41477-020-0695-2; pmid: 32601420
- S. D. Clouse, M. Langford, T. C. McMorris, A brassinosteroid-insensitive mutant in *Arabidopsis thaliana* exhibits multiple defects in growth and development. *Plant Physiol.* **111**, 671–678 (1996). doi: 10.1104/pp.111.3.671; pmid: 8754677
- Y. Hacham et al., Brassinosteroid perception in the epidermis controls root meristem size. *Development* **138**, 839–848 (2011). doi: 10.1242/dev.061804; pmid: 21270053
- T. M. Nolan, N. Vukašinović, D. Liu, E. Russinova, Y. Yin, Brassinosteroids: Multidimensional Regulators of Plant Growth, Development, and Stress Responses. *Plant Cell* **32**, 295–318 (2020). doi: 10.1105/tpc.19.00335; pmid: 31776234
- J. Li, P. Nagpal, V. Vitart, T. C. McMorris, J. Chory, A role for brassinosteroids in light-dependent development of *Arabidopsis*. *Science* **272**, 398–401 (1996). doi: 10.1126/science.272.5260.398; pmid: 8602526
- M.-P. González-García et al., Brassinosteroids control meristem size by promoting cell cycle progression in *Arabidopsis* roots. *Development* **138**, 849–859 (2011). doi: 10.1242/dev.057331; pmid: 21270057
- A. Caño-Delgado et al., BRL1 and BRL3 are novel brassinosteroid receptors that function in vascular differentiation in *Arabidopsis*. *Development* **131**, 5341–5351 (2004). doi: 10.1242/dev.01403; pmid: 15486337
- T. Kinoshita et al., Binding of brassinosteroids to the extracellular domain of plant receptor kinase BRL1. *Nature* **433**, 167–171 (2005). doi: 10.1038/nature03227; pmid: 15650741
- J. Li, J. Chory, A putative leucine-rich repeat receptor kinase involved in brassinosteroid signal transduction. *Cell* **90**, 929–938 (1997). doi: 10.1016/S0092-8674(00)80357-8; pmid: 9298904
- J. Li et al., BAK1, an *Arabidopsis* LRR receptor-like protein kinase, interacts with BRL1 and modulates brassinosteroid signaling. *Cell* **110**, 213–222 (2002). doi: 10.1016/S0092-8674(02)00812-7; pmid: 12150929
- Y. Yin et al., BES1 accumulates in the nucleus in response to brassinosteroids to regulate gene expression and promote stem elongation. *Cell* **109**, 181–191 (2002). doi: 10.1016/S0092-8674(02)00721-3; pmid: 12007405
- Z. Y. Wang et al., Nuclear-localized BZR1 mediates brassinosteroid-induced growth and feedback suppression of brassinosteroid biosynthesis. *Dev. Cell* **2**, 505–513 (2002). doi: 10.1016/S1534-5807(02)00153-3; pmid: 11970900
- Y. Sun et al., Integration of brassinosteroid signal transduction with the transcription network for plant growth regulation in *Arabidopsis*. *Dev. Cell* **19**, 765–777 (2010). doi: 10.1016/j.devcel.2010.10.010; pmid: 21074725
- X. Yu et al., A brassinosteroid transcriptional network revealed by genome-wide identification of BES1 target genes in *Arabidopsis thaliana*. *Plant J.* **65**, 634–646 (2011). doi: 10.1111/j.1365-313X.2010.04449.x; pmid: 2124652
- N. M. Clark et al., Integrated omics networks reveal the temporal signaling events of brassinosteroid response in *Arabidopsis*. *Nat. Commun.* **12**, 5858 (2021). doi: 10.1038/s41467-021-26165-3; pmid: 34615886
- R. Seyed Rahmani et al., Genome-wide expression and network analyses of mutants in key brassinosteroid signaling genes. *BMC Genomics* **22**, 465 (2021). doi: 10.1186/s12864-021-0778-w; pmid: 34157989
- H. Guo, L. Li, M. Aluru, S. Aluru, Y. Yin, Mechanisms and networks for brassinosteroid regulated gene expression. *Curr. Opin. Plant Biol.* **16**, 545–553 (2013). doi: 10.1016/j.pbi.2013.08.002; pmid: 23993372
- J. Fridman et al., Root growth is modulated by differential hormonal sensitivity in neighboring cells. *Genes Dev.* **28**, 912–920 (2014). doi: 10.1101/gad.239335.114; pmid: 24736847
- M. Ackerman-Lavert et al., Auxin requirements for a meristematic state in roots depend on a dual brassinosteroid function. *Curr. Biol.* **31**, 4462–4472.e6 (2021). doi: 10.1016/j.cub.2021.07.075; pmid: 34418341
- J. Villarrasa-Blasi et al., Regulation of plant stem cell quiescence by a brassinosteroid signaling module. *Dev. Cell* **30**, 36–47 (2014). doi: 10.1016/j.devcel.2014.05.020; pmid: 24981610
- K. Vragović et al., Transcriptome analyses capture of opposing tissue-specific brassinosteroid signals orchestrating root meristem differentiation. *Proc. Natl. Acad. Sci. U.S.A.* **112**, 923–928 (2015). doi: 10.1073/pnas.1417947112; pmid: 25561530
- I. Betegón-Putze et al., Precise transcriptional control of cellular quiescence by BRAVO/WOX5 complex in *Arabidopsis* roots. *Mol. Syst. Biol.* **17**, e9864 (2021). doi: 10.15252/msb.20209864; pmid: 34132490
- T. Asami et al., Characterization of brassinazole, a triazole-type brassinosteroid biosynthesis inhibitor. *Plant Physiol.* **123**, 93–100 (2000). doi: 10.1104/pp.123.1.93; pmid: 10806228
- M. D. Grove et al., Brassinolide, a plant growth-promoting steroid isolated from *Brassica napus* pollen. *Nature* **281**, 216–217 (1979). doi: 10.1038/2812160
- R. Shahani et al., A single-cell *Arabidopsis* root atlas reveals developmental trajectories in wild-type and cell identity mutants. *Dev. Cell* **57**, 543–560.e9 (2022). doi: 10.1016/j.devcel.2022.01.008; pmid: 3514336
- V. B. Ivanov, J. G. Dubrovsky, Longitudinal zonation pattern in plant roots: Conflicts and solutions. *Trends Plant Sci.* **18**, 237–243 (2013). doi: 10.1016/j.tplants.2012.10.002; pmid: 2312304
- E. Salvi, R. Di Mambro, S. Sabatini, Dissecting mechanisms in root growth from the transition zone perspective. *J. Exp. Bot.* **71**, 2390–2396 (2020). doi: 10.1093/jxb/eraa079; pmid: 32064533
- T. Denyer et al., Spatiotemporal Developmental Trajectories in the *Arabidopsis* Root Revealed Using High-Throughput Single-Cell RNA Sequencing. *Dev. Cell* **48**, 840–852.e5 (2019). doi: 10.1016/j.devcel.2019.02.022; pmid: 30913408
- J. Chaiwanon, Z.-Y. Wang, Spatiotemporal brassinosteroid signaling and antagonism with auxin pattern stem cell dynamics in *Arabidopsis* roots. *Curr. Biol.* **25**, 1031–1042 (2015). doi: 10.1016/j.cub.2015.02.046; pmid: 25866388
- P. E. Verslues, T. Longkumer, Siz1 and activity of the root meristem: A key for drought resistance and a key model of drought-related signaling. *Physiol. Plant.* **174**, e13622 (2022). doi: 10.1111/plp.13622; pmid: 34988997
- T. Longkumer, C.-Y. Chen, M. Bianucci, G. B. Bhaskara, P. E. Verslues, Spatial differences in stoichiometry of EGR phosphatase and Microtubule-associated Stress Protein 1 control root meristem activity during drought stress. *Plant Cell* **34**, 742–758 (2022). doi: 10.1093/plc/kocab290; pmid: 34865106
- D. Dietrich et al., Root hydrotropism is controlled via a cortex-specific growth mechanism. *Nat. Plants* **3**, 17057 (2017). doi: 10.1038/nplants.2017.57; pmid: 28481327
- R. Miao et al., Low ABA concentration promotes root growth and hydrotropism through relief of ABA INSENSITIVE 1-mediated inhibition of plasma membrane H⁺-ATPase 2. *Sci. Adv.* **7**, eabd4113 (2021). doi: 10.1126/sciadv.abd4113; pmid: 33731345
- L. Xie, C. Yang, X. Wang, Brassinosteroids can regulate cellulose biosynthesis by controlling the expression of CESA genes in *Arabidopsis*. *J. Exp. Bot.* **62**, 4495–4506 (2011). doi: 10.1093/jxb/erl164; pmid: 21617247
- G. Schieberinger et al., Optimal-Transport Analysis of Single-Cell Gene Expression Identifies Developmental Trajectories in Reprogramming. *Cell* **176**, 928–943.e22 (2019). doi: 10.1016/j.cell.2019.02.026; pmid: 30849376
- Y. Yin et al., A new class of transcription factors mediates brassinosteroid-regulated gene expression in *Arabidopsis*. *Cell* **120**, 249–259 (2005). doi: 10.1016/j.cell.2004.11.044; pmid: 15680330
- M. K. Zhipanova et al., Helix-loop-helix/basic helix-loop-helix transcription factor network represses cell elongation in *Arabidopsis* through an apparent incoherent feed-forward loop. *Proc. Natl. Acad. Sci. U.S.A.* **111**, 2824–2829 (2014). doi: 10.1073/pnas.1400203111; pmid: 24505057
- M. A. Moreno-Risueno et al., Transcriptional control of tissue formation throughout root development. *Science* **350**, 426–430 (2015). doi: 10.1126/science.aad1171; pmid: 26494755
- E. Henriksson et al., Homeodomain leucine zipper class I genes in *Arabidopsis*: Expression patterns and phylogenetic relationships. *Plant Physiol.* **139**, 509–518 (2005). doi: 10.1104/pp.105.063461; pmid: 16055682
- J. Mattsson, E. Söderman, M. Svensson, C. Borkird, P. Engström, A new homeobox-leucine zipper gene from *Arabidopsis thaliana*. *Plant Mol. Biol.* **18**, 1019–1022 (1992). doi: 10.1007/BF00019223; pmid: 1349836
- N. Vukašinović et al., Local brassinosteroid biosynthesis enables optimal root growth. *Nat. Plants* **7**, 619–632 (2021). doi: 10.1038/s41477-021-00917-x; pmid: 34007032
- D. M. Friedrichsen, C. A. Joazeiro, J. Li, T. Hunter, J. Chory, Brassinosteroid-insensitive-1 is a ubiquitously expressed leucine-rich repeat receptor serine/threonine kinase. *Plant Physiol.* **123**, 1247–1256 (2000). doi: 10.1104/pp.123.4.1247; pmid: 10938344
- Z. He et al., Perception of brassinosteroids by the extracellular domain of the receptor kinase BRL1. *Science* **288**, 2360–2363 (2000). doi: 10.1126/science.288.5475.2360; pmid: 10875920
- N. G. Irani et al., Fluorescent castasterone reveals BRI1 signaling from the plasma membrane. *Nat. Chem. Biol.* **8**, 583–589 (2012). doi: 10.1038/nchembio.958; pmid: 22561410
- M. Graeff et al., A single-cell morpho-transcriptomic map of brassinosteroid action in the *Arabidopsis* root. *Mol. Plant* **14**, 1985–1999 (2021). doi: 10.1016/j.molp.2021.07.021; pmid: 34358681
- Y. Fridman et al., The root meristem is shaped by brassinosteroid control of cell geometry. *Nat. Plants* **7**, 1475–1484 (2021). doi: 10.1038/s41477-021-01014-9; pmid: 3478271
- Y. H. Kang, A. Breda, C. S. Hardtke, Brassinosteroid signaling directs formative cell divisions and protophloem differentiation in *Arabidopsis* root meristems. *Development* **144**, 272–280 (2017). doi: 10.1242/dev.145623; pmid: 28096215
- M. Graeff, S. Rana, P. Marhava, B. Moret, C. S. Hardtke, Local and Systemic Effects of Brassinosteroid Perception in

- Developing Phloem. *Curr. Biol.* **30**, 1626–1638.e3 (2020). doi: [10.1016/j.cub.2020.02.029](https://doi.org/10.1016/j.cub.2020.02.029); pmid: [32220322](https://pubmed.ncbi.nlm.nih.gov/32220322/)
55. P. Barbier de Reuille *et al.*, MorphoGraphX: A platform for quantifying morphogenesis in 4D. *eLife* **4**, e05864 (2015). doi: [10.7554/eLife.05864](https://doi.org/10.7554/eLife.05864); pmid: [25946108](https://pubmed.ncbi.nlm.nih.gov/25946108/)
56. S. Strauss *et al.*, Using positional information to provide context for biological image analysis with MorphoGraphX 2.0. *eLife* **11**, e72601 (2022). doi: [10.7554/eLife.72601](https://doi.org/10.7554/eLife.72601); pmid: [35510843](https://pubmed.ncbi.nlm.nih.gov/35510843/)
57. F. Bou Daher *et al.*, Anisotropic growth is achieved through the additive mechanical effect of material anisotropy and elastic asymmetry. *eLife* **7**, e38161 (2018). doi: [10.7554/eLife.38161](https://doi.org/10.7554/eLife.38161); pmid: [30226465](https://pubmed.ncbi.nlm.nih.gov/30226465/)
58. T. I. Baskin, O. E. Jensen, On the role of stress anisotropy in the growth of stems. *J. Exp. Bot.* **64**, 4697–4707 (2013). doi: [10.1093/jxb/ert176](https://doi.org/10.1093/jxb/ert176); pmid: [23913952](https://pubmed.ncbi.nlm.nih.gov/23913952/)
59. E. Oh *et al.*, Cell elongation is regulated through a central circuit of interacting transcription factors in the Arabidopsis hypocotyl. *eLife* **3**, e03031 (2014). doi: [10.7554/eLife.03031](https://doi.org/10.7554/eLife.03031); pmid: [24867218](https://pubmed.ncbi.nlm.nih.gov/24867218/)
60. K. Kamimoto *et al.*, Dissecting cell identity via network inference and in silico gene perturbation. *Nature* **614**, 742–751 (2023). doi: [10.1038/s41586-022-05688-9](https://doi.org/10.1038/s41586-022-05688-9); pmid: [36755098](https://pubmed.ncbi.nlm.nih.gov/36755098/)
61. F. D. Ariel, P. A. Manavella, C. A. Dezar, R. L. Chan, The true story of the HD-Zip family. *Trends Plant Sci.* **12**, 419–426 (2007). doi: [10.1016/j.tplants.2007.08.003](https://doi.org/10.1016/j.tplants.2007.08.003); pmid: [17698401](https://pubmed.ncbi.nlm.nih.gov/17698401/)
62. M. F. Perotti, P. A. Ribone, J. V. Cabello, F. D. Ariel, R. L. Chan, ATHB23 participates in the gene regulatory network controlling root branching, and reveals differences between secondary and tertiary roots. *Plant J.* **100**, 1224–1236 (2019). doi: [10.1111/tpj.14511](https://doi.org/10.1111/tpj.14511); pmid: [31444832](https://pubmed.ncbi.nlm.nih.gov/31444832/)
63. A. T. Silva, P. A. Ribone, R. L. Chan, W. Ligterink, H. W. M. Hilhorst, A Predictive Coexpression Network Identifies Novel Genes Controlling the Seed-to-Seeding Phase Transition in *Arabidopsis thaliana*. *Plant Physiol.* **170**, 2218–2231 (2016). doi: [10.1104/pp.15.01704](https://doi.org/10.1104/pp.15.01704); pmid: [26888061](https://pubmed.ncbi.nlm.nih.gov/26888061/)
64. P. A. Ribone, M. Capella, R. L. Chan, Functional characterization of the homeodomain leucine zipper I transcription factor ATHB13 reveals a crucial role in *Arabidopsis* development. *J. Exp. Bot.* **66**, 5929–5943 (2015). doi: [10.1093/jxb/erv302](https://doi.org/10.1093/jxb/erv302); pmid: [26136262](https://pubmed.ncbi.nlm.nih.gov/26136262/)
65. J. C. Harris, M. Hrmova, S. Lopato, P. Langridge, Modulation of plant growth by HD-Zip class I and II transcription factors in response to environmental stimuli. *New Phytol.* **190**, 823–837 (2011). doi: [10.1111/j.1469-8137.2011.03733.x](https://doi.org/10.1111/j.1469-8137.2011.03733.x); pmid: [21517872](https://pubmed.ncbi.nlm.nih.gov/21517872/)
66. M. Shibata *et al.*, GTL1 and DF1 regulate root hair growth through transcriptional repression of *ROOT HAIR DEFECTIVE 6-LIKE 4* in *Arabidopsis*. *Development* **145**, dev159707 (2018). doi: [10.1242/dev.159707](https://doi.org/10.1242/dev.159707); pmid: [29439132](https://pubmed.ncbi.nlm.nih.gov/29439132/)
67. M. Shibata *et al.*, GTL1 is required for a robust root hair growth response to avoid nutrient overloading. *bioRxiv* 2021.06.27.450011 [Preprint] (2021). doi: [10.1101/2021.06.27.450011](https://doi.org/10.1101/2021.06.27.450011)
68. L. Li *et al.*, *Arabidopsis* MYB30 is a direct target of BES1 and cooperates with BES1 to regulate brassinosteroid-induced gene expression. *Plant J.* **58**, 275–286 (2009). doi: [10.1111/j.1365-313X.2008.03778.x](https://doi.org/10.1111/j.1365-313X.2008.03778.x); pmid: [19170933](https://pubmed.ncbi.nlm.nih.gov/19170933/)
69. K. Mabuchi *et al.*, MYB30 links ROS signaling, root cell elongation, and plant immune responses. *Proc. Natl. Acad. Sci. U.S.A.* **115**, E4710–E4719 (2018). doi: [10.1126/science.aaz7614](https://doi.org/10.1126/science.aaz7614); pmid: [32299946](https://pubmed.ncbi.nlm.nih.gov/32299946/)
70. A. Gupta, A. Rico-Medina, A. I. Caño-Delgado, The physiology of plant responses to drought. *Science* **368**, 266–269 (2020). doi: [10.1126/science.aaz7614](https://doi.org/10.1126/science.aaz7614); pmid: [32299946](https://pubmed.ncbi.nlm.nih.gov/32299946/)
71. B. O. R. Bargmann *et al.*, A map of cell type-specific auxin responses. *Mol. Syst. Biol.* **9**, 688 (2013). doi: [10.1038/msb.2013.40](https://doi.org/10.1038/msb.2013.40); pmid: [24022006](https://pubmed.ncbi.nlm.nih.gov/24022006/)
72. E. Shani *et al.*, Gibberellins accumulate in the elongating endodermal cells of *Arabidopsis* root. *Proc. Natl. Acad. Sci. U.S.A.* **110**, 4834–4839 (2013). doi: [10.1073/pnas.1300436110](https://doi.org/10.1073/pnas.1300436110); pmid: [23382232](https://pubmed.ncbi.nlm.nih.gov/23382232/)
73. S. Ubeda-Tomás *et al.*, Root growth in *Arabidopsis* requires gibberellin/DELLA signalling in the endodermis. *Nat. Cell Biol.* **10**, 625–628 (2008). doi: [10.1038/nclb1726](https://doi.org/10.1038/nclb1726); pmid: [18425113](https://pubmed.ncbi.nlm.nih.gov/18425113/)
74. Y. Geng *et al.*, A spatio-temporal understanding of growth regulation during the salt stress response in *Arabidopsis*. *Plant Cell* **25**, 2132–2154 (2013). doi: [10.1105/tpc.113.112896](https://doi.org/10.1105/tpc.113.112896); pmid: [23898029](https://pubmed.ncbi.nlm.nih.gov/23898029/)
75. A. S. Iyer-Pascuzzi *et al.*, Cell identity regulators link development and stress responses in the *Arabidopsis* root. *Dev. Cell* **21**, 770–782 (2011). doi: [10.1016/j.devcel.2011.09.009](https://doi.org/10.1016/j.devcel.2011.09.009); pmid: [22014526](https://pubmed.ncbi.nlm.nih.gov/22014526/)
76. M. Ackerman-Lavert, S. Savaldi-Goldstein, Growth models from a brassinosteroid perspective. *Curr. Opin. Plant Biol.* **53**, 90–97 (2020). doi: [10.1016/j.pbi.2019.10.008](https://doi.org/10.1016/j.pbi.2019.10.008); pmid: [31809963](https://pubmed.ncbi.nlm.nih.gov/31809963/)
77. Y. Jaillais, Y. Belkhadir, E. Balsemão-Pires, J. L. Dangl, J. Chory, Extracellular leucine-rich repeats as a platform for receptor/coreceptor complex formation. *Proc. Natl. Acad. Sci. U.S.A.* **108**, 8503–8507 (2011). doi: [10.1073/pnas.1103556108](https://doi.org/10.1073/pnas.1103556108); pmid: [21464298](https://pubmed.ncbi.nlm.nih.gov/21464298/)
78. J. Stuttmann *et al.*, Highly efficient multiplex editing: One-shot generation of 8× *Nicotiana benthamiana* and 12× *Arabidopsis* mutants. *Plant J.* **106**, 8–22 (2021). doi: [10.1111/tpj.15197](https://doi.org/10.1111/tpj.15197); pmid: [33577114](https://pubmed.ncbi.nlm.nih.gov/33577114/)
79. R. Grützner *et al.*, High-efficiency genome editing in plants mediated by a Cas9 gene containing multiple introns. *Plant Commun.* **2**, 100135 (2020). doi: [10.1016/j.xpc.2020.100135](https://doi.org/10.1016/j.xpc.2020.100135); pmid: [33898975](https://pubmed.ncbi.nlm.nih.gov/33898975/)
80. C.-W. Hsu, R. Shahani, T. M. Nolan, P. N. Benfey, U. Ohler, Protocol for fast scRNA-seq raw data processing using scKBB and non-arbitrary quality control with COPilot. *STAR Protoc.* **3**, 101729 (2022). doi: [10.1101/xpro.2022.101729](https://doi.org/10.1101/xpro.2022.101729); pmid: [36181683](https://pubmed.ncbi.nlm.nih.gov/36181683/)
81. T. Stuart *et al.*, Comprehensive Integration of Single-Cell Data. *Cell* **177**, 1888–1902.e21 (2019). doi: [10.1016/j.cell.2019.05.031](https://doi.org/10.1016/j.cell.2019.05.031); pmid: [3178118](https://pubmed.ncbi.nlm.nih.gov/3178118/)
82. H. L. Crowell *et al.*, muscat detects subpopulation-specific state transitions from multi-sample multi-condition single-cell transcriptomics data. *Nat. Commun.* **11**, 6077 (2020). doi: [10.1038/s41467-020-19894-4](https://doi.org/10.1038/s41467-020-19894-4); pmid: [33257685](https://pubmed.ncbi.nlm.nih.gov/33257685/)
83. K. Van den Berghe *et al.*, Trajectory-based differential expression analysis for single-cell sequencing data. *Nat. Commun.* **11**, 1201 (2020). doi: [10.1038/s41467-020-14766-3](https://doi.org/10.1038/s41467-020-14766-3); pmid: [32139671](https://pubmed.ncbi.nlm.nih.gov/32139671/)
84. T. Nolan, C.-W. Hsu, L. Greenstreet, tmnolan/Brassinosteroid-gene-regulatory-networks-at-cellular-resolution: Brassinosteroid gene regulatory networks at cellular resolution in the *Arabidopsis* root, version 1.0, Zenodo (2022); doi: [10.5281/zenodo.7489359](https://doi.org/10.5281/zenodo.7489359)
85. T. Nolan, Brassinosteroid gene regulatory networks at cellular resolution in the *Arabidopsis* root, data set, Zenodo (2022); doi: [10.5281/zenodo.7489389](https://doi.org/10.5281/zenodo.7489389)

ACKNOWLEDGMENTS

The authors thank H. Belcher and M. Perkins Jacobs for technical assistance; N. Devos and Duke GCB for sequencing services; N. Vangheluwe, T. Beeckman, and T. B. Jacobs (VIB-UGent) for CRISPR-TSKO advice; and K. Sugimoto for *gtl1* and *df1* seeds.

Funding: This study was supported by the Howard Hughes Medical Institute (P.N.B.); National Institutes of Health MIRA 1R35GM131725 (P.N.B.); National Science Foundation Postdoctoral Research Fellowships in Biology Program grant IOS-2010686 (T.M.N.); National Institutes of Health NRSA postdoctoral fellowship 1F32GM136030-01 (R.S.); Research Foundation-Flanders GO0212IN (E.R.); Research Foundation-Flanders Postdoctoral fellowships nos. 12R7822N and 12R7819N (N.V.); US Department of Agriculture National Institute of Food and Agriculture fellowship 2021-67034-35139 (I.W.T.); National Science Foundation grant MCB 1818160 (Y.Y.); Deutsche Forschungsgemeinschaft International Research Training Group 2403 (C.-W.H. and U.O.); a Career Award at the Scientific Interface from the Burroughs Wellcome Fund (L.G., M.H., and G.S.); a New Frontiers in Research Fund (NFRF) exploration grant (L.G., M.H., A.A., and G.S.); a Natural Sciences and Engineering Research Council of Canada (NSERC) discovery grant (L.G., M.H., A.A., and G.S.); and a project grant from the Canadian Institute of Health Research (L.G., M.H., A.A., and G.S.). **Author contributions:** Conceptualization: T.M.N., N.V., C.-W.H., E.R., and P.N.B. Methodology: T.M.N., N.V., C.-W.H., J.Z., P.S., I.V., A.B., and P.W. Investigation: T.M.N., N.V., R.S., I.W.T., J.Z., P.S., I.V., A.B., and P.W. Data analysis: C.-W.H., T.M.N., L.G., M.H., A.A., and G.S. Writing: T.M.N., C.-W.H., N.V., R.S., I.W.T., E.R., and P.N.B. Supervision: P.N.B., E.R., U.O., G.S., and Y.Y. **Competing interests:** P.N.B. is the cofounder and chair of the Scientific Advisory Board of Hi Fidelity Technologies, a company that works on crop root growth. The authors declare no other competing interests. **Data and materials availability:** scRNA-seq data have been deposited at Gene Expression Omnibus (GEO) (accession no. GSE212230) and can be visualized through an interactive browser at <https://shiny.mdc-berlin.de/ARVEX/>. All data are available in the manuscript or the supplementary materials or are deposited at Zenodo (84, 85). **License information:** Copyright © 2023 the authors, some rights reserved; exclusive licensee American Association for the Advancement of Science. No claim to original US government works. <https://www.science.org/about/science-licenses-journal-article-reuse>. This article is subject to HHMI's Open Access to Publications policy. HHMI lab heads have previously granted a nonexclusive CC BY 4.0 license to the public and a sublicensable license to HHMI in their research articles. Pursuant to those licenses, the author-accepted manuscript of this article can be made freely available under a CC BY 4.0 license immediately upon publication.

SUPPLEMENTARY MATERIALS

science.org/doi/10.1126/science.adf4721

Materials and Methods

Figs. S1 to S21

References (86–130)

MDAR Reproducibility Checklist

Movie S1

Data S1 to S6

View/request a protocol for this paper from Bio-protocol.

Submitted 24 October 2022; accepted 9 February 2023
10.1126/science.adf4721